Mechanics of Advanced Composite Structures 11 (2024) 149 – 158


Semnan University

Mechanics of Advanced Composite Structures

journal homepage: http://MACS.journals.semnan.ac.ir

# Static Buckling and Free Vibration Analysis of Bi-Dimensional FG Metal Ceramic Porous Beam

**Y. Shabani, P. Mehdianfar, K. Khorshidi ***

*Department of Mechanical Engineering, Faculty of Engineering, Arak University, Arak, 38156-88349, Iran*

**KEYWORDS**

Porosity;
Computational analysis;
2D-FGM;
Composite materials;
Buckling.

**ABSTRACT**

This study presents an analytical solution for static buckling and free vibration analysis of bi-dimensional functionally graded (2D-FG) metal-ceramic porous beams. To achieve this goal, equations of motion for the beam are derived by using Hamilton's principle and then the derived equations were solved in the framework of Galerkin's well-known analytical method for solution of equations. The material properties of the beam are variable along with thickness and length according to the power-law function. During the fabrication of functionally graded materials (FGMs), porosities may occur due to technical problems causing micro-voids to appear. Detailed mathematical derivations are presented and numerical investigations are performed, while emphasis is placed on investigating the effect of various parameters such as FG power indexes along both directions of thickness and length, porosity, and slenderness ratios (L/h), on the non-dimensional frequency and static buckling of the beam based on new higher deformation beam theory. The accuracy of the proposed model is validated based on comparisons of the results with the accepted studies. According to the result in both buckling and vibration analysis, the presented modified transverse shear stress along the thickness has shown closer consequences in comparison with TBT.

## 1. Introduction

In recent years, a new class of composite materials formed that contained two or more phases which are known as functionally graded materials (FGMs). FGMs are made of two or more substances whose characteristics vary continuously from one direction to another. The performances and advantages of FGMs have led to their increasing use in many sectors including hi-tech industries, aerospace, naval, automotive, and civil structures[1]. An important application of FGM in structural components is in beams and beam structures. To support the growing use of FGM beams, the study of their vibration behavior becomes necessary. In recent years, the analysis of the free vibration of FGM beams has been performed using different analytical and numerical methods[2]. buckling and free vibration of a curved Timoshenko FG microbeam is studied by Rahmani et al. [3] based on strain gradient theory (SGT) theory. Compared to conventional materials, porous materials possess both remarkable design flexibility and significant applicability across diverse fields. Consequently, numerous researchers have dedicated their efforts to exploring various porous structures. For instance, Ghasemi and Meskini [4] conducted an investigation into the free vibration analysis of porous laminated rotating circular cylindrical shells. Several studies have been carried out on the behaviors of functionally graded material in recent years [5-10]. Atashipour et al. [11] developed a closed-form 2D elasticity solution for stresses and displacements of a curved FG beam subjected to a shear force. Among the earliest investigators in this field, Masjedi et al. [12], conducted a large deflection of functionally graded porous beams based on a geometrically exact theory. The buckling behavior of engineering structures made of advanced materials has been investigated by many researchers[13-18]. Buckling of Sandwich Structures with Metamaterials Core Integrated

* Corresponding author. Tel.: +98-86-32625720 ; Fax: +98-86-32625721
*E-mail address:* k-khorshidi@araku.ac.ir

DOI: 10.22075/macs.2023.29847.1476
Received 2023-02-08; Received in revised form 2023-08-18; Accepted 2023-09-08.

by Graphene Nanoplatelets Reinforced Polymer Composite was analyzed by Shabani and Khorshidi[19]. The analytical solution presented by Dym and Williams [20] can be used to estimate the buckling behavior of curved beams. The nondeterministic vibration frequencies and mode shapes of FG porous beams were investigated by Gao et al. [21] using a hybrid Chebyshev surrogate model with a discrete singular convolution method. Large amplitude nonlinear vibration analysis of functionally graded porous Timoshenko beams is examined by Ebrahimi and Zia [22]. Chen et al. [23] investigated free vibration and transient analyses of functionally graded piezoelectric materials curved Timoshenko beams in their work. Mahmoodabadi et al. [24] used a multi-objective optimization process based on the genetic algorithm to study damping the vibrations of a piezo-actuating composite beam. The Peridynamics analytical solutions for the buckling load of beams with various boundary conditions were introduced by Yang et al. [25]. Ly et al. [26] used different hybrid ML models to predict the critical buckling load of I-shaped cellular steel beams with circular openings.

In this study, the effects of variable L/h, porosity coefficient, and gradient indexes in two directions on natural frequency and critical buckling load of 2D-FG porous beams have been investigated. Young's modulus, mass density, and Poisson's ratio of the beam are assumed to vary along the thickness and length of the beam according to power-laws form and also, they are influenced by the porosity. In this study to achieve better accuracy, modified transverse shear stress has been presented and compared with other theories. In the following, the higher-order governing equations are derived by using Hamilton's principle. In the end, the Galerkin method is employed to solve them, and the non-dimensional frequencies and critical buckling loads are obtained.

## 2. Problem and Formulation

### *2.1. Two Dimensionally Functionally Graded Porous Beams*

Consider a beam as shown in Fig. 1. with length L, width b, and thickness h, with Cartesian coordinate system O(x y z) which the origin of coordinate system O is chosen at the left of the beam. The Mechanical properties of the beam, such as Young's modulus E(x, z), shear modulus G(x, z), Poisson's modulus υ(x, z) and mass density ρ(x, z) with the material properties can be varying along length and thickness like Fig. 1.

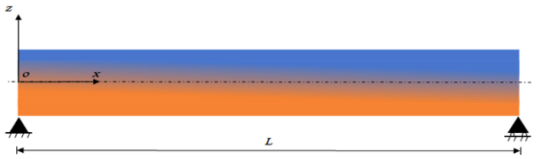


**Fig. 1.** Geometry of 2D-FG beam.

The effective material properties(P) can be expressed by using the rule of mixture:

$$P(x,z) = P_C R_C(x,z) + P_m R_m(x,z) \quad (1)$$

$$R_C(x,z) + R_m(x,z) = 1 \quad (2)$$

where $P_c$ and $P_m$ are epitomes of mechanical properties and $R_c$ and $R_m$ are volume fractions of ceramic and metal. Substitution of Eq. (2) into Eq. (1), the material properties of the 2D-FG beam are obtained as [27]:

$$P(x,z) = (P_C - P_m)R_C + P_m \quad (3)$$

As shown in Fig. 2, it is assumed that the porosities in the x and z directions are distributed uniformly. The effective material properties of the even porosity are defined as:

$$P(x,z) = (P_C - P_m)R_C + P_m - \left(\frac{\eta}{2}(P_C + P_m)\right) \quad (4)$$

where $\eta$ is a porous parameter or porosity volume fraction.

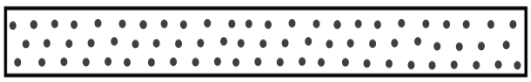

**Fig. 2.** Porosity of beam.

The assumed beam is graded from metal at the lower left corner edge to ceramic at the top right corner edge (Fig. 1). The volume fraction of ceramic material is given by:

$$R_C(x,z) = \left(\frac{x}{L}\right)^{k_x}\left(\frac{z}{h}+\frac{1}{2}\right)^{k_z} \quad (5)$$

The $k_x$ and $k_z$ are the power-law of the beam which ascertain properties in length and thickness direction. The mechanical properties of the 2D-FG porous beam can be written as [28]:

$$E(x,z) = (E_C - E_m)\left(\frac{x}{L}\right)^{k_x}\left(\frac{z}{h}+\frac{1}{2}\right)^{k_z} + E_m - \left(\frac{\eta}{2}(E_C + E_m)\right) \quad (6a)$$

$$\rho(x,z) = (\rho_C - \rho_m)\left(\frac{x}{L}\right)^{k_x}\left(\frac{z}{h}+\frac{1}{2}\right)^{k_z} + \rho_m - \left(\frac{\eta}{2}(\rho_C + \rho_m)\right) \quad (6b)$$

$$\upsilon(x,z)=(\upsilon_c-\upsilon_m)\left(\frac{x}{L}\right)^{k_x}\left(\frac{z}{h}+\frac{1}{2}\right)^{k_z}+\upsilon_m-\left(\frac{\eta}{2}(\upsilon_c+\upsilon_m)\right) \quad (6c)$$

## 2.2. Mathematical Modeling

The displacement filed the present shear deformation beam theories, are given as [29]:

$$u_x(x,z)=u(x)-g(z)\frac{\partial w(x)}{\partial x}+f(z)\varphi(x) \quad (7a)$$

$$u_z(x,z)=w(x) \quad (7b)$$

where u(x) and w(x) respectively represent the axial and transverse displacements for the mid-access, and φ is the rotation of the cross-sections. Assuming infinitesimal deformations, strain-displacement relations are[30]:

$$\varepsilon_{xx}=\frac{\partial u(x)}{\partial x}-g(z)\frac{\partial^2 w(x)}{\partial x^2}+f(z)\frac{\partial\varphi(x)}{\partial x} \quad (8a)$$

$$\gamma_{xz}=-\frac{\partial g(z)}{\partial z}\frac{\partial w(x)}{\partial x}+\frac{\partial f(z)}{\partial z}\varphi(x)+\frac{\partial w(x)}{\partial x} \quad (8b)$$

The stress-strain relations by using Hook's law can be defined as follows:

$$\sigma_{xx}=E(x,z)\varepsilon_{xx} \quad (9a)$$

$$\tau_{xz}=k_S G(x,z)\gamma_{xz} \quad (9b)$$

E and G represent the modulus of elasticity and shear moduli, respectively, while ks denotes the shear correction factor. Where the shear modulus (G) is [31]:

$$G(x,z)=\frac{E(x,z)}{2(1+\upsilon(x,z))} \quad (10)$$

Hamilton's principle is employed to extract equations of motion [32, 33].

$$\int_0^t(\delta U-\delta T)\,dt=0 \quad (11)$$

where U and T are the strain and kinetic energy, respectively of the beam. $\delta$ is the variation operator. The strain energy of the beam(U) is calculated as follows [34, 35]:

$$U=\frac{1}{2}\int_V\sigma_{ij}\varepsilon_{ij}dV=\frac{1}{2}\int_V(\sigma_{xx}\varepsilon_{xx}+\tau_{xx}\gamma_{xx})dV \quad (12)$$

Finally, variation of strain energy with respect to u(x), w(x) and φ(x) is shown as.

$$\delta U=\frac{1}{2}\int_A\left[-\delta u\frac{\partial A_{xx}}{\partial x}-\delta w\left(\frac{\partial^2 B_{xx}}{\partial x^2}-\frac{\partial S_{xz}}{\partial x}+\frac{\partial A_{xz}}{\partial x}\right)-\delta\varphi\left(\frac{\partial D_{xx}}{\partial x}-T_{xz}\right)\right]dA \quad (13)$$

where $A_{xx}$, $A_{xz}$, $B_{xx}$, $D_{xx}$, $S_{xz}$, and $T_{xz}$ are defined by:

$$(A_{xx},A_{xz})=-\int_{-h/2}^{h/2}(\sigma_{xx},\tau_{xz})\,dz \quad (14a)$$

$$(B_{xx},D_{xx})=\int_{-h/2}^{h/2}(g(z),f(z))\,\sigma_{xx}\,dz \quad (14b)$$

$$(S_{xz},T_{xz})=\int_{-h/2}^{h/2}\left(\frac{\partial g(z)}{\partial z},\frac{\partial f(z)}{\partial z}\right)\tau_{xz}\,dz \quad (14c)$$

The kinetic energy is obtained as [36]:

$$T=\frac{1}{2}\int_V\rho\left[\dot{u}_x^2+\dot{u}_z^2\right]dV \quad (15)$$

The inertia coefficients appearing in Eq. 19 can be defined as:

$$(I_1,I_2,I_3,I_4,I_5,I_6)=-\int_{-h/2}^{h/2}\rho(1,g(z),f(z),g(z)f(z),g(z)^2,f(z)^2)\,dz \quad (16)$$

Finally, the total variation of kinetic energy associated with the sandwich beam in the integral form as:

$$\delta T=\frac{1}{2}\int_A\left[\left(-I_1\ddot{u}+I_2\frac{\partial\ddot{w}}{\partial x}-I_3\ddot{\varphi}\right)\delta u+\left(-I_3\ddot{u}+I_4\frac{\partial\ddot{w}}{\partial x}-I_6\ddot{\varphi}\right)\delta\varphi-\left(I_2\frac{\partial\ddot{u}}{\partial x}-I_5\frac{\partial^2\ddot{w}}{\partial x^2}+I_4\frac{\partial\ddot{\varphi}}{\partial x}-I_1\ddot{w}\right)\delta w\right]dA \quad (17)$$

By substituting strain energy Eq. (13) and kinetic energy Eq. (17) into Hamilton's principal Eq. (11), equations of motion may be expressed as Eqs. (18a) – (18c).

$$\delta u:\frac{\partial A_{xx}}{\partial x}=I_1\ddot{u}-I_2\frac{\partial\ddot{w}}{\partial x}+I_3\ddot{\varphi} \quad (18a)$$

$$\delta w:\frac{\partial^2 B_{xx}}{\partial x^2}-\frac{\partial S_{xz}}{\partial x}+\frac{\partial A_{xz}}{\partial x}=I_2\frac{\partial\ddot{u}}{\partial x}-I_5\frac{\partial^2\ddot{w}}{\partial x^2}+I_4\frac{\partial\ddot{\varphi}}{\partial x}+I_1\ddot{w} \quad (18b)$$

$$\delta\varphi:\frac{\partial D_{xx}}{\partial x}-T_{xz}=I_3\ddot{u}-I_4\frac{\partial\ddot{w}}{\partial x}+I_6\ddot{\varphi} \quad (18c)$$

### 2.3. Analytical Solution

To obtain the theoretical solution, the Galerkin method is considered. According to this method, the displacements functions u(x, t), w(x, t) and φ(x, t) are assumed as follows[37]:

$$u(x,t)=\sum_{m=1}^{K}\left[\Upsilon_m \bar{u}_m\right]e^{i\omega t} \quad (19a)$$

$$w(x,t)=\sum_{n=1}^{K}\left[\Psi_n \bar{w}_n\right]e^{i\omega t} \quad (19b)$$

$$\varphi(x,t)=\sum_{j=1}^{K}\left[\Phi_j \bar{\varphi}_j\right]e^{i\omega t} \quad (19c)$$

where $\bar{u}_m$, $\bar{w}_n$ and $\bar{\varphi}_j$ are unknown coefficients that will be determined. i = $\sqrt{-1}$, K denotes the order of series and $\omega$ is the natural frequency. $\Upsilon_m(x)$, $\Psi_n(x)$ and $\Phi_j(x)$ are the admissible functions that satisfy the fully clamped boundary conditions.

$$\Upsilon_m(x)=(L-x)^{q_0}x^{(m+p_0)-1} \quad (20a)$$

$$\Psi_n(x)=(L-x)^{q_0}x^{(n+p_0)-1} \quad (20b)$$

$$\Phi_j(x)=(L-x)^{q_0}x^{(j+p_0)-1} \quad (20c)$$

Free vibration analysis of the bi-dimensional functionally graded sandwich beam can be computed from Eq. (21a)[38]. Also, the amount of critical buckling loads will be calculated by Eq. (21b):

$$\left\{[K]-\omega^2[M]\right\}\{\lambda\}=0 \quad (21a)$$

$$\left\{[K]-N_{cr}\left[K_g\right]\right\}\{\lambda\}=0 \quad (21b)$$

where M is the global mass matrix, K is the stiffness matrix and unknown coefficients of Eq. (21) is $\{\lambda\}$.

## 3. Numerical Results and Discussion

In this section, the free vibration of the 2D-FG porous beam with respect to porosity coefficients ($\eta$) is studied. Functionally graded material composed of a mixture of alumina and steel as ceramic and metal respectively with the material. Their properties are given in Table 1. The influence of different slenderness ratios, L/h = 5, 10, 15, and 20 on the non-dimensional natural frequency are investigated. The shear correction factor for TBT theory is considered as ks = 5/6 [39].

**Table 1.** Properties of materials[37]

| Material | Elasticity module (E) | Mass density (ρ) | Poisson's ratio (υ) |
|---|---|---|---|
| Alumina | 380 | 3800 | 0.23 |
| Steel | 70 | 2700 | 0.23 |

The dimensionless fundamental frequency and critical buckling load are defined as Eq. 22.

$$\bar{\omega}=\omega^2\sqrt{\frac{\rho_c A}{E_c I}} \quad (22a)$$

$$\bar{N}_{cr}=N_{cr}\frac{12L^2}{E_c h^3} \quad (22b)$$

where I represent the moment of inertia and A represents the area of the cross-section of the beam.

$$I=\frac{A.h^2}{12} \quad (23)$$

In this research, the solution is calculated for different the power-law index between 0 and 10 moreover, porosity coefficients are taken as $\eta = 0, 0.1,$ and 0.2. The total thickness of the beam (h) is constant and it is 0.1 m. The function indexes (p0 and q0), are taken as 2 for satisfying the clamped-clamped boundary condition. Besides, g(z) and f(z) are related parameters to the beam's theory, as they take as 0 and z for TBT, and z and $z\left(\frac{4}{h}-\frac{16z^2}{3h^3}\right)$ for NHOBT [40], respectively. Validation of our formulation and the results are obtained and compared with the results of Ref. [41], [42], and [43]. In Table 2, the first frequency of FG porous less beam with L/h = 5 and $k_x$ = 0 are calculated and they will be compared with references. To verify our new theory, the natural frequency of the FG beam with a greater slender ratio in Table 3 is calculated.

In addition, another comparison with ref [41] and [43] is presented to show the accuracy of the new higher shear deformation beam theory to calculate the critical buckling load. The mechanical properties of the pure beam have changed along the z direction and the ratio of beam's length to height is 10. The results are written in Table 4.

The amounts of Ncr of the FG beam with NHOBT and L/h = 5 are reported in Table 5. By checking both tables, it is clear that there is accuracy and agreement between the references and the present study. Thus, the results of natural frequencies and critical buckling loads will be published under effective parameters such as L/h, porosity (η), and functionally graded power indexes ($k_x$ and $k_z$).

The results of non-dimensional frequencies of a two-dimensional functionally graded porous beam with several η, $k_x$, and $k_z$ by using two theories are written in Table 6. The amount of ϖ has been reduced by approximately 37% by changing $k_z$ from 0 to 8. On the other hand, the variation of $k_x$ has affected ϖ by around 34%, indicating that $k_z$ has a greater impact on the results. Additionally, by changing η from 0 to 0.2, the amount of ϖ has increased by approximately 3%.

The amount of Ncr under changing $k_x$, $k_z$, and η with TBT and NHOBT is calculated and the consequences are written in Table 7. By changing $k_z$ and $k_x$ between 0 to 8, the amount of Ncr has reduced by about 76 and 69 % respectively. The factor with the greatest impact on the results is $k_z$, with approximately 7% more effect. Furthermore, the Ncr decreased by about 11% with increasing η from 0 to 0.2.

**Table 2.** Comparison of the dimensionless natural frequencies (l/h = 5 and η = 0)

| | kz = 0 | kz = 1 | kz = 2 | kz = 5 | kz = 10 |
|---|---|---|---|---|---|
| Present (NHOBT) | 10.2285 | 8.0969 | 7.3290 | 6.6448 | 6.3042 |
| Present (TBT) | 10.2579 | 8.1098 | 7.3750 | 6.7128 | 6.4759 |
| Thuc et al. HOBT [41] | 10.0678 | 7.9522 | 7.1801 | 6.4961 | 6.1662 |
| Thuc et al. FOBT [41] | 9.9984 | 7.9015 | 7.1901 | 6.6447 | 6.3161 |
| Simsek HOBT [42] | 10.0705 | 7.9503 | 7.1767 | 6.4935 | 6.1652 |
| Simsek FOBT [42] | 10.0344 | 7.9253 | 7.2113 | 6.6676 | 6.3406 |

**Table 3.** Comparison of the dimensionless natural frequencies (l/h = 20 and η = 0)

| | kz = 0 | kz = 1 | kz = 2 | kz = 5 | kz = 10 |
|---|---|---|---|---|---|
| Present (NHOBT) | 12.2418 | 9.4918 | 8.6778 | 8.2159 | 7.9342 |
| Thuc et al. HOBT [41] | 12.2228 | 9.4328 | 8.5994 | 8.1460 | 7.8862 |
| Thuc et al. FOBT [41] | 12.2202 | 9.4311 | 8.6047 | 8.1698 | 7.9115 |
| Simsek HOBT [42] | 12.2238 | 9.4315 | 8.5975 | 8.1446 | 7.8858 |
| Simsek FOBT [42] | 12.2235 | 9.4314 | 8.6040 | 8.1699 | 7.9128 |

**Table 4.** Comparison of the results of critical buckling load (l/h = 10 and η = 0)

| | kz = 0 | kz = 1 | kz = 2 | kz = 5 | kz = 10 |
|---|---|---|---|---|---|
| Present (NHOBT) | 194.4026 | 98.8053 | 76.8331 | 62.9629 | 56.4158 |
| Li and Batra [43] | 195.3400 | 98.7490 | 76.9800 | 64.0960 | 57.7080 |
| Thuc et al. FOBT [41] | 195.3730 | 98.7923 | 77.0261 | 64.1324 | 57.7329 |
| Thuc et al. HOBT [41] | 195.3610 | 98.7868 | 76.6677 | 62.9786 | 56.5971 |

**Table 5.** Comparison of the results of critical buckling load (l/h = 5 and η = 0)

| | kz = 0 | kz = 1 | kz = 2 | kz = 5 | kz = 10 |
|---|---|---|---|---|---|
| Present (NHOBT) | 152.1990 | 79.8063 | 61.2369 | 47.116 | 41.1128 |
| Li and Batra [43] | 154.3500 | 80.4980 | 62.6140 | 50.3840 | 44.2670 |
| Thuc et al. FOBT [41] | 154.4150 | 80.5480 | 62.6616 | 50.4207 | 44.2946 |
| Thuc et al. HOBT [41] | 154.5500 | 80.6087 | 61.7925 | 47.7562 | 41.8042 |

**Table 6.** First non-dimensional frequency (ϖ) of 2D-FG porous beam for various kx, kz, and η (L/h = 10).

| Theory | η | kz | kx | | | | | |
|---|---|---|---|---|---|---|---|---|
| | | | 0 | 1 | 2 | 4 | 6 | 8 |
| TBT | 0 | 0 | 21.6960 | 17.0553 | 15.6524 | 14.5606 | 14.0223 | 13.6403 |
| | | 1 | 16.8500 | 14.3819 | 13.6517 | 13.0863 | 12.7849 | 12.5764 |
| | | 2 | 15.3637 | 13.6340 | 13.0914 | 12.6367 | 12.4165 | 12.2903 |
| | | 4 | 14.6350 | 13.2308 | 12.7760 | 12.3834 | 12.1918 | 12.0892 |
| | | 6 | 14.3520 | 13.0449 | 12.6168 | 12.2521 | 12.0960 | 11.9658 |
| | | 8 | 14.1373 | 12.8873 | 12.4975 | 12.1511 | 12.0043 | 11.9063 |
| NHOBT | 0 | 0 | 21/1618 | 16/6429 | 15/3731 | 14/2928 | 13/7558 | 13/3948 |
| | | 1 | 16/5051 | 14/0453 | 13/3743 | 12/8050 | 12/5325 | 12/3574 |
| | | 2 | 15/0571 | 13/3139 | 12/8158 | 12/3854 | 12/1817 | 12/0524 |
| | | 4 | 14/2740 | 12/8894 | 12/4747 | 12/1139 | 11/9551 | 11/8567 |
| | | 6 | 13/9665 | 12/6941 | 12/3101 | 11/9907 | 11/8451 | 11/7547 |
| | | 8 | 13/7419 | 12/5464 | 12/1924 | 11/8892 | 11/7570 | 11/6799 |

| | | | | | | | | |
|---|---|---|---|---|---|---|---|---|
| TBT | 0.1 | 0 | 21.9998 | 16.7114 | 15.0772 | 13.6923 | 13.0121 | 12.5896 |
| | | 1 | 16.5388 | 13.6219 | 12.7145 | 12.0111 | 11.6668 | 11.4278 |
| | | 2 | 14.6162 | 12.6623 | 12.0187 | 11.4848 | 11.2217 | 11.0879 |
| | | 4 | 13.6436 | 12.1432 | 11.6160 | 11.1728 | 10.9759 | 10.8546 |
| | | 6 | 13.3410 | 11.9406 | 11.4468 | 11.0374 | 10.8555 | 10.7441 |
| | | 8 | 13.1444 | 11.7965 | 11.3355 | 10.9355 | 10.7829 | 10.6676 |
| NHOBT | 0.1 | 0 | 22/3579 | 16/9650 | 15/3647 | 14/0096 | 13/3560 | 12/9310 |
| | | 1 | 16/7512 | 13/8084 | 12/9738 | 12/2489 | 11/9219 | 11/7106 |
| | | 2 | 14/8641 | 12/8713 | 12/2623 | 11/7220 | 11/4849 | 11/3378 |
| | | 4 | 13/9234 | 12/3669 | 11/8677 | 11/4237 | 11/2257 | 11/1112 |
| | | 6 | 13/6599 | 12/1858 | 11/7091 | 11/2917 | 11/1181 | 11/0058 |
| | | 8 | 13/4683 | 12/0397 | 11/5834 | 11/1987 | 11/0331 | 10/9345 |
| TBT | 0.2 | 0 | 22.3718 | 16.2578 | 13.9010 | 12.1407 | 11.3053 | 10.7474 |
| | | 1 | 16.0382 | 12.4432 | 11.2190 | 10.2780 | 9.8109 | 9.5400 |
| | | 2 | 13.4114 | 11.1096 | 10.2812 | 9.5863 | 9.2764 | 9.0820 |
| | | 4 | 11.8584 | 10.3262 | 9.7099 | 9.1750 | 8.9410 | 8.8175 |
| | | 6 | 11.4574 | 10.0734 | 9.5067 | 9.0297 | 8.8242 | 8.6936 |
| | | 8 | 11.3014 | 9.9231 | 9.3867 | 8.9382 | 8.7464 | 8.6273 |
| NHOBT | 0.2 | 0 | 22/7021 | 16/3349 | 14/2677 | 12/4383 | 11/6037 | 11/0778 |
| | | 1 | 16/2534 | 12/5477 | 11/4541 | 10/4811 | 10/0477 | 9/7799 |
| | | 2 | 13/6285 | 11/2567 | 10/4767 | 9/7967 | 9/4873 | 9/3149 |
| | | 4 | 12/0916 | 10/4981 | 9/9149 | 9/3829 | 9/1574 | 9/0258 |
| | | 6 | 11/7261 | 10/2714 | 9/7284 | 9/2452 | 9/0443 | 8/9243 |
| | | 8 | 11/5545 | 10/1302 | 9/6076 | 9/1525 | 8/9648 | 8/8529 |

**Table 7.** Critical buckling load (Ncr) of 2D-FG porous beam for various kx, kz, and η (L/h = 10).

| Theory | η | kz | kx | | | | | |
|---|---|---|---|---|---|---|---|---|
| | | | 0 | 1 | 2 | 4 | 6 | 8 |
| TBT | 0 | 0 | 201.3001 | 101.2443 | 73/3782 | 56/8435 | 51/2608 | 48/3640 |
| | | 1 | 101.8384 | 66.6279 | 55/4769 | 47/7935 | 44/9744 | 43/4770 |
| | | 2 | 79.3865 | 58.3191 | 50/8079 | 45/2804 | 43/1927 | 42/0855 |
| | | 4 | 68.2815 | 53.5313 | 47/9427 | 43/6789 | 42/0411 | 41/1664 |
| | | 6 | 64.3308 | 51.4026 | 46/5823 | 42/8864 | 41/4587 | 40/6963 |
| | | 8 | 61.6250 | 49.8626 | 45/5830 | 42/2954 | 41/0188 | 40/3319 |
| NHOBT | 0 | 0 | 195/3779 | 97/2664 | 71/2192 | 55/4709 | 50/1329 | 47/3546 |
| | | 1 | 99/2310 | 64/5146 | 53/9762 | 46/6343 | 43/9498 | 42/5304 |
| | | 2 | 77/1877 | 56/4267 | 49/3866 | 44/1401 | 42/1719 | 41/1327 |
| | | 4 | 65/7422 | 51/5953 | 46/4741 | 42/5032 | 40/9942 | 40/1957 |
| | | 6 | 61/5646 | 49/4644 | 45/1055 | 41/7020 | 40/4027 | 39/7119 |
| | | 8 | 58/8715 | 47/9899 | 44/1322 | 41/1171 | 39/9625 | 39/3461 |
| TBT | 0.1 | 0 | 189/7017 | 86/5973 | 58/2271 | 42/5622 | 37/4739 | 34/8816 |
| | | 1 | 88/0537 | 52/9688 | 41/9996 | 34/7625 | 32/1893 | 30/8440 |
| | | 2 | 64/0969 | 44/5446 | 37/5045 | 32/4321 | 30/5622 | 29/5826 |
| | | 4 | 52/5693 | 39/8829 | 34/8210 | 30/9839 | 29/5379 | 28/7694 |
| | | 6 | 49/1145 | 38/0454 | 33/6697 | 30/3341 | 29/0618 | 28/3879 |
| | | 8 | 46/9595 | 36/7694 | 32/8503 | 29/8570 | 28/7108 | 28/1008 |
| NHOBT | 0.1 | 0 | 184/1132 | 82/7353 | 56/4400 | 41/5326 | 36/6694 | 34/1715 |
| | | 1 | 85/8718 | 51/1773 | 40/8558 | 33/9401 | 31/4780 | 30/1892 |
| | | 2 | 62/4375 | 43/0432 | 36/4529 | 31/6364 | 29/8622 | 28/9356 |
| | | 4 | 50/6270 | 38/3560 | 33/7335 | 30/1575 | 28/8153 | 28/1133 |
| | | 6 | 46/8667 | 36/4948 | 32/5662 | 29/4938 | 28/3337 | 27/7230 |
| | | 8 | 44/6357 | 35/2597 | 31/7613 | 29/0213 | 27/9825 | 27/4327 |
| TBT | 0.2 | 0 | 178/0717 | 70/4071 | 40/9069 | 26/8716 | 22/6228 | 20/5068 |
| | | 1 | 73/6780 | 38/2597 | 27/4892 | 20/9948 | 18/8072 | 17/6832 |
| | | 2 | 47/4333 | 29/7059 | 23/3508 | 18/9993 | 17/4592 | 16/6723 |
| | | 4 | 34/6064 | 25/0341 | 20/8595 | 17/7380 | 16/5918 | 16/0017 |
| | | 6 | 31/5006 | 23/5343 | 19/9695 | 17/2607 | 16/2562 | 15/7359 |
| | | 8 | 30/0213 | 22/6233 | 19/3964 | 16/9431 | 16/0272 | 15/5484 |
| NHOBT | 0.2 | 0 | 172/8112 | 66/3052 | 39/5456 | 26/1841 | 22/1330 | 20/0973 |
| | | 1 | 71/9500 | 36/7506 | 26/6959 | 20/4944 | 18/4025 | 17/3281 |
| | | 2 | 46/3571 | 28/6013 | 22/6763 | 18/5411 | 17/0741 | 16/3237 |
| | | 4 | 33/4452 | 23/9716 | 20/1835 | 17/2666 | 16/1973 | 15/6521 |
| | | 6 | 30/0084 | 22/4247 | 19/2647 | 16/7747 | 15/8535 | 15/3803 |
| | | 8 | 28/3175 | 21/5147 | 18/6904 | 16/4552 | 15/6238 | 15/1932 |

The beam is made of two-dimensional functionally graded material; thus, it has been influenced by FG power indexes in x ($k_x$) and z ($k_z$) directions. The critical buckling loads (Ncr) and the natural frequencies (ϖ) of the beam are related to the $k_x$ and $k_z$. In Figure 3a, the relation between ϖ and FG power indexes in a porous less beam is shown, the ratio of length to the height of the beam is considered as 10. In Figure 3b, the effect of FG power indexes on Ncr of the porous beam is under new theory (NHOBT) with η = 0.2 and L/h = 10 illustrated. Generally, the amount of Ncr and ϖ have reduced with increasing the FG power indexes. However, Ncr has been affected more than ϖ by changing $k_x$ and $k_z$. In the high amount of FG power indexes the variations of Ncr have been moved to near 0. On the other hand, the ϖ has been diminished continuously by reducing the $k_x$ and $k_z$. Power indexes affect how material properties vary along the length and thickness directions, which influence their stiffness and mass distribution. A higher FG power index reduces the effective stiffness and increases the effective mass of a beam.

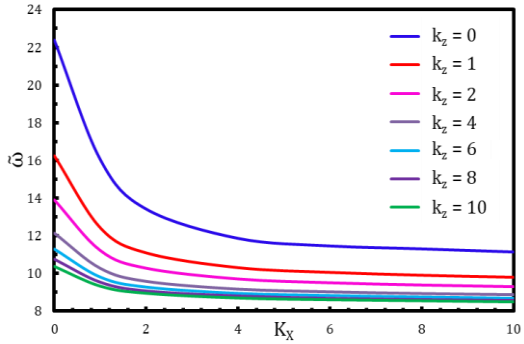


**Fig. 3a.** Non-dimensional frequency of 2D-FG porous beam for various $k_z$ and $k_x$ (TBT, L/h = 10 and η = 0)

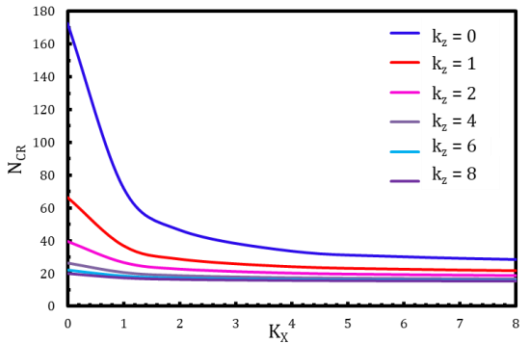


**Fig. 3b.** Critical buckling load of 2D-FG porous beam for various $k_z$ and $k_x$ (NHOBT, L/h = 10 and η = 0.2)

The impact of various ratios of the beam's spin to its height on ϖ and Ncr is shown in Figure 4. A beam with n = 0.1 and $k_x$ = 1 is used to analyze the three amounts of L/h = 5, 10, and 20 on the ϖ in the first part of the Figure. A direct connection is seen between the amount of L/h and the ϖ. Additionally, the same study on Ncr has been conducted under unique conditions using a new theory. The results of this study are plotted in Figure 4b and the amount of Ncr has been rose by growing the L/h from 5 to 20. Also, the effect of L/h = 5 on the Ncr and ϖ is higher than 10 and 20. Reducing the strain energy will decrease the bending moment of the beam, so when the L/h is going to be diminished, the amount of Ncr and ϖ will be reduced. A higher slenderness ratio means a longer and thinner beam, which is more flexible and less stiff than a shorter and thicker beam.

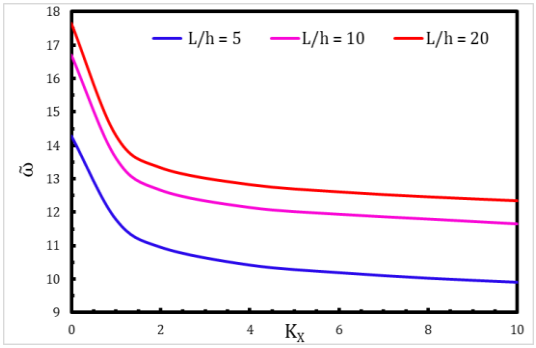


**Fig. 4a.** Comparison of non-dimensional frequency of 2D-FG porous beam for various slenderness ratios (L/h) (η = 0.1 and $k_x$ = 1)

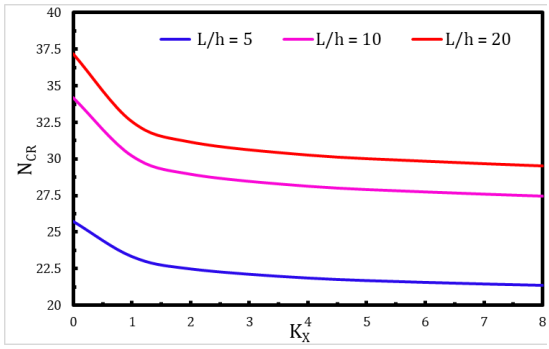


**Fig. 4b.** Comparison of Critical buckling load of 2D-FG porous beam for various height to span ratios (L/h) (NHOBT, η = 0.1 and $k_x$ = 1)

Another important and effective parameter is porosity. Figure 5 shows the effect of η = 0, 0.1, and 0.2 on the Ncr and ϖ. When the amount of η is 0, the beam does not have any porosity. In the constant $k_z$ and $k_z$, the ϖ has shown an inverse direction with η so as to by increasing the η, ϖ has fallen. The same relation is seen between η and Ncr, however, the effect on Ncr is bolder than on ϖ. By reducing the stiffness of the beam, the amount of ϖ and Ncr will be influenced and decreased. Porosity affects the material density and strength along the thickness direction of beams, which in turn affects their stiffness and mass. Higher porosity means more voids or holes in the material, which reduces its weight and resistance to deformation. A higher porosity reduces the effective stiffness and increases the effective mass of a beam under both axial and transverse loading, which lowers its critical buckling load and natural frequency.

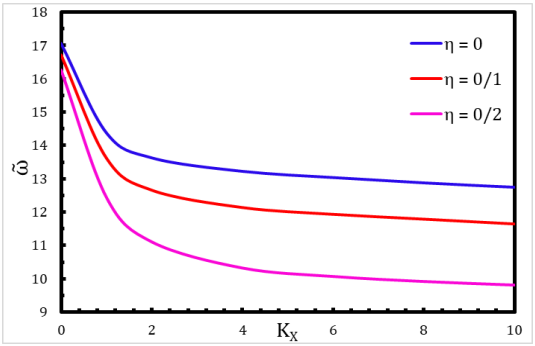


**Fig. 5a.** Effect of various porosity(η) on non-dimensional frequency of 2D-FG porous beam (L/h = 10 and kx = 1)

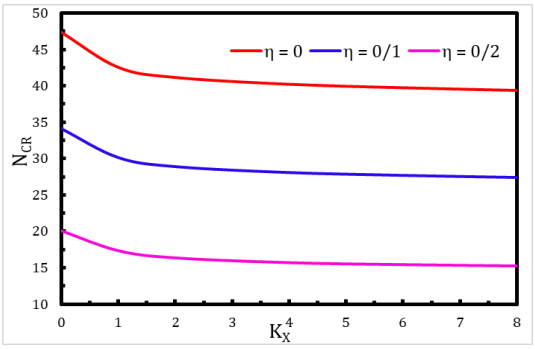


**Fig. 5b.** Effect of various porosity(η) on Critical buckling load of 2D-FG porous beam (NHOBT, L/h = 10 and kx = 8)

## 4. Conclusions

In this research paper, we have investigated the impact of various parameters, including porosity (η), slenderness ratios (L/h), and power-law indexes (kx and kz) in both axial and thickness directions, on the natural frequencies and critical buckling load of 2D-FG porous beams. We have utilized a new higher-order beam theory to analyze these effects.

Our findings demonstrate that the power-law indexes (kx and kz) play a significant role in determining the natural frequencies. Increasing the FG power indexes leads to a decrease in the values of the natural frequencies (Ncr) and the critical buckling load (ϖ). This can be explained by the change in material properties along the beam's axial and thickness directions. The power-law indexes alter the distribution of the constituent materials, affecting their stiffness and density. Higher power-law indexes result in a more significant variation of material properties, leading to decreased natural frequencies and critical buckling loads. In the case of high power-law indexes, the variations in Ncr do not exhibit significant changes. Additionally, when considering a constant value for kx and kz, we observe an inverse relationship between the porosity (η) and ϖ. As η increases, ϖ decreases, and the same trend is observed between η and Ncr. This behavior can be attributed to the presence of voids or pores within the material. The presence of voids weakens the overall structural integrity and reduces the effective stiffness of the beam. As a result, the natural frequencies decrease, and the critical buckling load is diminished. Furthermore, frequencies and critical buckling loads are more sensitive to porosity in high power-law indexes. A direct connection is seen between the amount of L/h and the ϖ. The amount of Ncr has been rose by growing the L/h from 5 to 20. Also, the effect of L/h = 5 on the Ncr and ϖ is higher than 10 and 20.

These findings provide valuable insights into the behavior of bi-dimensional FG metal ceramic porous beams and highlight the importance of considering porosity, slenderness ratios, and power-law indexes in their design and analysis. Further research in this area can contribute to the development of more efficient and reliable structures with improved performance characteristics.

## Conflicts of Interest

The author declares that there is no conflict of interest regarding the publication of this manuscript. In addition, the authors have entirely observed the ethical issues, including plagiarism, informed consent, misconduct, data fabrication and/or falsification, double publication and/or submission, and redundancy.

## References

[1] Sharma, N.K. & Bhandari, M., 2018. Applications of functionally graded materials (fgms). *International journal of engineering research and technology, 2*.

[2] Ramteke, P.M. & Panda, S.K., 2023. Computational modelling and experimental challenges of linear and nonlinear analysis of porous graded structure: A comprehensive review. *Archives of Computational Methods in Engineering, 30* (5), pp.3437-3452.

[3] Rahmani, O., Hosseini, S.a.H., Ghoytasi, I. & Golmohammadi, H., 2016. Buckling and free vibration of shallow curved micro/nano-beam based on strain gradient theory under thermal loading with temperature-dependent properties. *Applied Physics A, 123* (1), pp.4.

[4] Ghasemi, A.R. & Meskini, M., 2019. Free vibration analysis of porous laminated rotating circular cylindrical shells. *Journal of Vibration and Control, 25* (18), pp.2494-2508.

[5] Khorshidi, K., Bahrami, M., Karimi, M. & Ghasemi, M., 2020. A theoretical approach for flexural behavior of fg vibrating micro-plates with piezoelectric layers considering a hybrid length scale parameter. *Journal of*

*Theoretical and Applied Vibration and Acoustics, 6* (1), pp.51-68.

[6] Zhu, C. & Xu, S.P., 2018. Nonlinear free vibration analysis of fg tubes conveying fluid. *Zhendong yu Chongji/Journal of Vibration and Shock, 37*, pp.195-201 and 247.

[7] Bouafia, H., Abdelbaki, C., Bousahla, A., Bourada, F., Heireche, H., Tounsi, A., Benrahou, K., Tounsi, A., Al-Zahrani, M. & Hussain, M., 2021. Natural frequencies of fgm nanoplates embedded in an elastic medium. *Advances in Nano Research, 11*.

[8] Hidayat, M.I.P., 2022. A meshless thermal modelling for functionally graded porous materials under the influence of temperature dependent heat sources. *Engineering Analysis with Boundary Elements, 145*, pp.188-210.

[9] Alavi, S.K., Ayatollahi, M.R., Petrů, M. & Koloor, S.S.R., 2022. On the dynamic response of viscoelastic functionally graded porous plates under various hybrid loadings. *Ocean Engineering, 264*, pp.112541.

[10] El Khouddar, Y., Adri, A., Outassafte, O., Rifai, S. & Benamer, R., 2021. Non-linear forced vibration analysis of piezoelectric functionally graded beams in thermal environment. *International Journal of Engineering, 34* (11), pp.2387-2397.

[11] Atashipour, S.R., Nasr, A. & Fadaee, M., 2010. An elasticity solution for static analysis of functionally graded curved beam subjected to a shear force. *International Journal of Engineering, 23* (2), pp.169-178.

[12] Khaneh Masjedi, P., Maheri, A. & Weaver, P.M., 2019. Large deflection of functionally graded porous beams based on a geometrically exact theory with a fully intrinsic formulation. *Applied Mathematical Modelling, 76*, pp.938-957.

[13] Emam, S. & Lacarbonara, W., 2022. A review on buckling and postbuckling of thin elastic beams. *European Journal of Mechanics - A/Solids, 92*, pp.104449.

[14] Zhao, H., Li, K., Han, M., Zhu, F., Vázquez-Guardado, A., Guo, P., Xie, Z., Park, Y., Chen, L., Wang, X., Luan, H., Yang, Y., Wang, H., Liang, C., Xue, Y., Schaller, R.D., Chanda, D., Huang, Y., Zhang, Y. & Rogers, J.A., 2019. Buckling and twisting of advanced materials into morphable 3d mesostructures. *Proceedings of the National Academy of Sciences, 116* (27), pp.13239-13248.

[15] Ghasemi, A.R., Kiani, S. & Tabatabaeian, A., 2020. Buckling analysis of fml cylindrical shells under combined axial and torsional loading. *Mechanics Of Advanced Composite Structures, 7* (2), pp.263-270.

[16] Ghasemi, A.R. & Soleymani, M., 2021. A new efficient buckling investigation of functionally graded cnt/fiber/polymer/metal composite panels exposed to hydrostatic pressure considering simultaneous manufacturing-induced agglomeration and imperfection issues. *The European Physical Journal Plus, 136* (12), pp.1220.

[17] Bridjesh, P., Geetha, N.K. & Reddy, G.C.M., 2023. On numerical investigation of buckling in two-directional porous functionally graded beam using higher order shear deformation theory. *Mechanics Of Advanced Composite Structures, 10* (2), pp.393-406.

[18] Reddy, G.C.M. & Kumar, N.V., 2023. Free vibration analysis of 2d functionally graded porous beams using novel higher-order theory. *Mechanics Of Advanced Composite Structures, 10* (1), pp.69-84.

[19] Shabani, Y. & Khorshidi, K., 2023. Buckling analysis of sandwich structures with metamaterials core integrated by graphene nanoplatelets reinforced polymer composite. *Mechanics Of Advanced Composite Structures, 10* (1), pp.1-10.

[20] Dym, C.L. & Williams, H.E., 2011. Stress and displacement estimates for arches. *Journal of structural engineering, 137* (1), pp.49-58.

[21] Gao, K., Li, R. & Yang, J., 2019. Dynamic characteristics of functionally graded porous beams with interval material properties. *Engineering Structures, 197*, pp.109441.

[22] Ebrahimi, F. & Zia, M., 2015. Large amplitude nonlinear vibration analysis of functionally graded timoshenko beams with porosities. *Acta Astronautica, 116*, pp.117-125.

[23] Chen, M., Chen, H., Ma, X., Jin, G., Ye, T., Zhang, Y. & Liu, Z., 2018. The isogeometric free vibration and transient response of functionally graded piezoelectric curved beam with elastic restraints. *Results in Physics, 11*, pp.712-725.

[24] Mahmoodabadi, M.J., Mortazavi Yazdi, S.M. & Barani, A., 2020. Vibration damping of piezo actuating composite beams based on the multi-objective genetic algorithm. *Journal of Theoretical and Applied Vibration and Acoustics, 6* (2), pp.325-336.

[25] Yang, Z., Naumenko, K., Altenbach, H., Ma, C.-C., Oterkus, E. & Oterkus, S., 2022. Beam

buckling analysis in peridynamic framework. *Archive of Applied Mechanics, 92*.

[26] Ly, H.-B., Le, T.-T., Le, L., Van Quan, T., Vương, L., Thi Vu, H.-L., Nguyen, Q. & Pham, B., 2019. Development of hybrid machine learning models for predicting the critical buckling load of i-shaped cellular beams. *Applied Sciences, 9*, pp.5458.

[27] Gupta, S. & Chalak, H.D., 2023. Buckling analysis of functionally graded sandwich beam based on third-order zigzag theory. *Mechanics Of Advanced Composite Structures, 10* (1), pp.55-68.

[28] Shahsavari, D., Shahsavari, M., Li, L. & Karami, B., 2018. A novel quasi-3d hyperbolic theory for free vibration of fg plates with porosities resting on winkler/pasternak/kerr foundation. *Aerospace Science and Technology, 72*, pp.134-149.

[29] Reddy, J.N., 2011. Microstructure-dependent couple stress theories of functionally graded beams. *Journal of the Mechanics and Physics of Solids, 59* (11), pp.2382-2399.

[30] Wattanasakulpong, N. & Chaikittiratana, A., 2015. Flexural vibration of imperfect functionally graded beams based on timoshenko beam theory: Chebyshev collocation method. *Meccanica, 50* (5), pp.1331-1342.

[31] Katili, A.M. & Katili, I., 2020. A simplified ui element using third-order hermitian displacement field for static and free vibration analysis of fgm beam. *Composite Structures, 250*, pp.112565.

[32] Ghasemi, A.R. & Mohandes, M., 2020. Free vibration analysis of micro and nano fiber-metal laminates circular cylindrical shells based on modified couple stress theory. *Mechanics of Advanced Materials and Structures, 27* (1), pp.43-54.

[33] Nejati, M., Ghasemi-Ghalebahman, A., Soltanimaleki, A., Dimitri, R. & Tornabene, F., 2019. Thermal vibration analysis of sma hybrid composite double curved sandwich panels. *Composite Structures, 224*, pp.111035.

[34] Khorshidi, K., Taheri, M. & Ghasemi, M., 2020. Sensitivity analysis of vibrating laminated composite rec-tangular plates in interaction with inviscid fluid using efast method. *Mechanics of Advanced Composite Structures, 7* (2), pp.219-231.

[35] Khorshid, K. & Farhadi, S., 2013. Free vibration analysis of a laminated composite rectangular plate in contact with a bounded fluid. *Composite Structures, 104*, pp.176-186.

[36] Shabani, Y. & Khorshidi, K., 2022. Free vibration analysis of rectangular doubly curved auxetic-core sandwich panels integrated with cnt-reinforced composite layers using galerkin method. *Journal of Science and Technology of Composites, 8* (3), pp.1686-1677.

[37] Elmeiche, A., Megueni, A. & Lousdad, A., 2016. Free vibration analysis of functionally graded nanobeams based on different order beam theories using ritz method. *Periodica Polytechnica Mechanical Engineering, 60* (4), pp.209-219.

[38] Khorshidi, K. & Shabani, Y., 2022. Free vibration analysis of sandwich plates with magnetorheological smart fluid core by using modified shear deformation theory. *Journal of Science and Technology of Composites*, pp.-.

[39] Şimşek, M. & Al-Shujairi, M., 2017. Static, free and forced vibration of functionally graded (fg) sandwich beams excited by two successive moving harmonic loads. *Composites Part B: Engineering, 108*, pp.18-34.

[40] Mehdianfar, P., Shabani, Y. & Khorshidi, K., 2022. Natural frequency of sandwich beam structures with two dimensional functionally graded porous layers based on novel formulations. *International Journal of Engineering, 35* (11), pp.2092-2101.

[41] Vo, T.P., Thai, H.-T., Nguyen, T.-K., Maheri, A. & Lee, J., 2014. Finite element model for vibration and buckling of functionally graded sandwich beams based on a refined shear deformation theory. *Engineering Structures, 64*, pp.12-22.

[42] Şimşek, M., 2010. Fundamental frequency analysis of functionally graded beams by using different higher-order beam theories. *Nuclear Engineering and Design, 240* (4), pp.697-705.

[43] Li, S.-R. & Batra, R.C., 2013. Relations between buckling loads of functionally graded timoshenko and homogeneous euler–bernoulli beams. *Composite Structures, 95*, pp.5-9.